

Viscoelastic Properties and Reinforcement Performance of the MoS₂ Nanotubes–polymer Composite

A. Jelen¹, V. Bukošek², J. Dolinšek^{1,3,4,*}

¹Solid State Physics Department, J. Stefan Institute, Ljubljana, Slovenia

²Department of Textiles, Faculty of Natural Sciences and Engineering, University of Ljubljana, Slovenia

³Faculty of Mathematics and Physics, University of Ljubljana, Slovenia

⁴EN–FIST Centre of Excellence, Slovenia

jani.dolinsek@ijs.si .

Abstract–We present viscoelastic properties and reinforcement performance of a polymer nanocomposite containing MoS₂ nanotubes. The MoS₂ nanotubes are mechanically strong and flexible, behaving as super shock absorbers and exceptional lubricants with very low friction coefficient and excellent wear resistance. Using Dynamic Mechanical Analysis, we have defined viscoelastic properties (the storage modulus E' , the loss modulus E'' , the phase lag δ and the length l) of the MoS₂–polymer nanocomposite coatings with different nanotubes concentrations. The glass transition temperature of the nanocomposites has shifted by $\Delta T_g \approx 10^\circ\text{C}$ towards higher temperatures. The $\tan \delta$ peak temperature T_δ and the temperatures T_{\max} and T_{\min} of the maximum elongation/contraction have shifted towards higher temperatures by the same amount. The main benefit of the MoS₂ nanotubes addition is a significant increase of the storage modulus E' within the temperature range suitable for mechanical loading, being roughly a factor of 2 larger than E' of the base coating without the MoS₂ nanotubes.

Keywords–Nanocomposites; MoS₂; nanotubes; Dynamic Mechanical Analysis

I. INTRODUCTION

Polymer matrix-based nanocomposites are involved in a range of applications including material reinforcement, barrier to permeation, flammability resistance, polymer blend compatibilization, biomedical tissue engineering, drug delivery/release applications, fuel cells, electronics, photovoltaics, sensors, antimicrobial and cosmetic applications [1]. The addition of nanosized particles to the polymer matrix results in a change of the glass transition temperature T_g , the degree of crystallinity and the crystallization rate, which affect the properties of the nanocomposite in a fundamental way. In the reinforcement application [2], a common reason for adding nanofillers to polymers is to increase the Young's modulus or stiffness, the strength and the toughness of the nanocomposite. Nanocomposite has also a weight advantage over the conventional glass-fiber reinforced composite. Moreover, while fibers reinforce only along a single axis in the direction of their alignment, nanoparticles generally reinforce in all directions. Surface finish of the nanocomposite is much better than that of the glass fiber, owing to the nanometer size of the particles. One of the disadvantages of adding fillers is that they generally decrease the ductility of polymers, i.e. elongation at break. The reduced ductility is more severe when the polymer matrix is below its glass transition, whereas it is less dramatic above T_g . Better reinforcement results are

generally obtained above T_g as it is easier to reinforce softer matrices.

There are four main system requirements for effective reinforcement of a nanocomposite by tube-type nanofillers (e.g. nanotubes, nanorods, nanoropes and nanofibers). These are:

(1) Large aspect ratio l/D , where l is the tube length and D its external diameter. In order to maximize the composite stiffness and strength, long tubes are generally required. However, long tubes are hard to disperse properly, so that one is faced with a trade-off. Similarly, low-diameter nanotubes give rise to greater surface area allowing maximization of interaction with the matrix. However, if the diameter gets too small, the maximum nanotube loading level (stress transfer) will be compromised. For these reasons there exist optimum diameter and length, with l typically of the order of a few μm and D of the order of 100 nm;

(2) Good dispersion, where the nanotubes must be uniformly dispersed to the level of isolated nanotubes individually coated with polymer. This is imperative in order to achieve efficient load transfer to the nanotube network and a uniform stress distribution. Any aggregation of the nanotubes due to poor dispersion is accompanied by a decrease in strength and modulus;

(3) Alignment is less crucial issue. For perfect alignment, the composite modulus is theoretically a factor of five larger than for random orientation. While alignment is necessary to maximize the strength and stiffness, aligned composites have very anisotropic mechanical properties, which may need to be avoided in bulk samples;

(4) the most important requirement for a nanotubes-reinforced composite is that external stresses applied to the composite as a whole are efficiently transferred to the nanotubes, allowing them to take a disproportionate share of the load. Upon application of an external stress, σ , the polymer matrix undergoes greater strain, ϵ , than the nanotube, because the nanotube modulus E_{NT} is much larger than the matrix modulus E_m and $\sigma = E\epsilon$. The result is that a shear stress field can be very large adjacent to the nanotube. It is this matrix shear stress at the interface that controls stress transfer to the nanotube. At some critical value of the interfacial shear stress, either the matrix in the vicinity of the interface or the matrix-nanotube bond will rupture, which results in debonding and consequent mechanical failure of the

nanocomposite. The critical value of the interfacial shear stress governs the maximum stress transfer to the nanotube. Good adhesion of the nanotubes to the matrix is thus necessary for efficient stress transfer.

Carbon nanotubes turned out to be superior reinforcement filler material for improving stiffness/strength of the nanocomposites [2]. Other nanofiller materials incorporated in polymer composites were also used for property enhancement [1]. These include exfoliated clays for improved stiffness/strength and permeability barrier, multi-walled carbon nanotubes for improved electrical conductivity, carbon black for improved strength, wear and abrasion, silver nanoparticles for antimicrobial application and electrically conductive ink and silica nanoparticles for viscosity control. In this paper we present processing and viscoelastic properties of a polymer nanocomposite by using MoS₂ nanotubes [3,4] as the filler material. The MoS₂ and the related WS₂ nanotubes and fullerene-like nanoparticles possess a rare combination of being mechanically very strong and flexible [5]. The Young's modulus of the MoS₂ nanoropes (composed of several nanotubes) was estimated to have its lower limit at 120 GPa [5]. The MoS₂ and WS₂ nanotubes behave as exceptional lubricants [6, 7], either solid-state or as additives to lubricating fluids, with very low friction coefficients (between 0.008 and 0.01) [8] and excellent wear resistance. The MoS₂ and the WS₂ nanoparticles were also shown to act as super shock absorbers at very high pressures [9], surviving shocks as high as 25 GPa. MoS₂ nanotubes can store relatively large amounts of hydrogen [10], having gaseous storage capacity of 1.2 wt. % hydrogen. The MoS₂ and WS₂ nanomaterials were also used in electronic devices [11] and as catalysts [12]. Their superior mechanical/tribological properties make them promising nanofillers in polymer-based nanocomposites for the reinforcement application. Using Dynamic Mechanical Analysis (DMA), we present viscoelastic properties of the MoS₂ nanotubes-polymer composite as a function of the temperature and concentration of the nanotubes.

II. NANOCOMPOSITE PROCESSING

The commercial MoS₂ nanotubes were supplied by Nanotul, d.o.o., Slovenia. The SEM secondary-electron micrograph of the nanotubes is shown in Fig. 1. The tube lengths range from a few up to 15 μ m, whereas their diameters are from 100 to 400 nm, assuring close to optimal aspect ratio l/D . A small fraction of smaller rods with lengths in the submicron range and diameters of about 100 nm is present as well. The small rods are attached to the larger ones. The nanotubes are flexible and can bend and twist. In some cases, the growth direction has changed discontinuously, producing zigzag structures. The nanotube edges are not perfectly closed, allowing better adhesion of the polymer because of more rough contact surface. The as-grown nanotubes show tendency to attach parallel to each other, forming sheaves of three or more nanotubes bound together.

In the first step of the nanocomposite processing, solvents, methacrylate monomers for polymerization, additives for light stabilization and UV absorption and a catalyst were added together. In the second step, MoS₂ nanotubes were added in volumetric fractions 0, 1, 3, 6, 12 and 15 vol. %, followed by ultrasonication for fine dispersion. The hardening step involved addition of hexamethylene diisocyanate for polymerization. All processing was performed at controlled room temperature (RT).

Nanocomposite coatings were produced on aluminum holders of 25 mm diameter for the SEM microscopy, wherefrom they could be later removed for testing with DMA. Freshly mixed components of the nanocomposite were deposited drop by drop with constant mixing. The coatings were left for 24 hours at RT for polymerization and solvents evaporation. The thickness of the coatings was typically about 280 μ m. Six coatings were produced altogether. The reference coating without the MoS₂ addition is denoted as the *base* in the following. The five nanocomposite coatings containing MoS₂ nanotubes are denoted as the base + vol. % of MoS₂ addition (i.e., base + 1 %, base + 3 %, etc.).

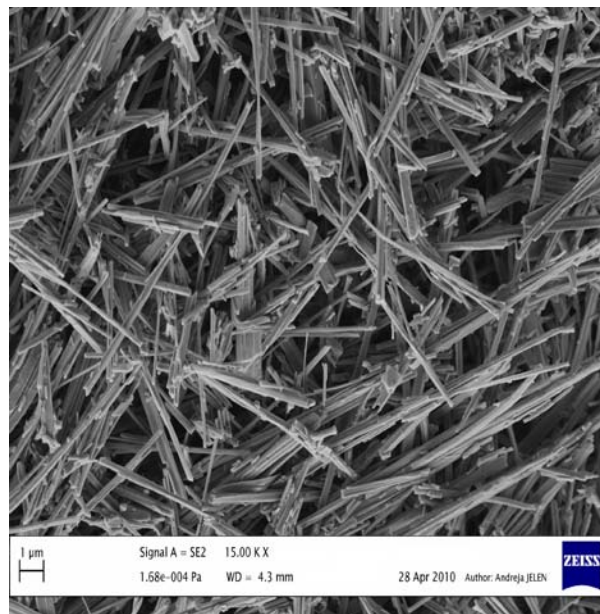


Fig. 1 SEM secondary-electron micrograph of the MoS₂ nanotubes

III. NANOCOMPOSITE CHARACTERIZATION BY MICROSCOPY TECHNIQUES

The microscopy characterization of the nanocomposite coatings was performed by Light Microscopy (LM) using optical stereo microscope Leica EZ4D with integrated CCD camera and imaging software Leica Microsystems LAS EZ, Scanning Electron Microscopy (SEM) using field-emission SEM Karl Zeiss Supra 35 VP and Transmission Electron Microscopy (TEM) using JEOL JEM-2100 TEM.

A. LM Characterization

Fig. 2 shows LM images of the six investigated coatings. The base coating is transparent, so that the shiny polished aluminum holder surface is seen underneath (Fig. 2a). The lines are scratches on the polished holder surface. By adding MoS₂ nanotubes, the coatings are gaining in optical density. At 1 % addition (Fig. 2b), the coating is still mostly transparent. Majority of the nanotubes have organized into groups of different sizes from sub-micron up to 100- μ m diameter (observed as black spots) that are distributed evenly over the sample. The base + 3 % coating is almost opaque (Fig. 2c). The groups of nanotubes are smaller and their distribution is denser, approaching more homogeneous distribution. A few scratches on the holder remain visible. The base + 6 % (Fig. 2d), base + 12 % (Fig. 2e) and base + 15 % (Fig. 2f) coatings have similar appearance, showing full coverage of the holder with no transparency any more, as a consequence of a homogeneous distribution of the nanotubes.

Inhomogeneities of the nanotubes distribution on the scale below the LM resolution of about 200 nm cannot be excluded.

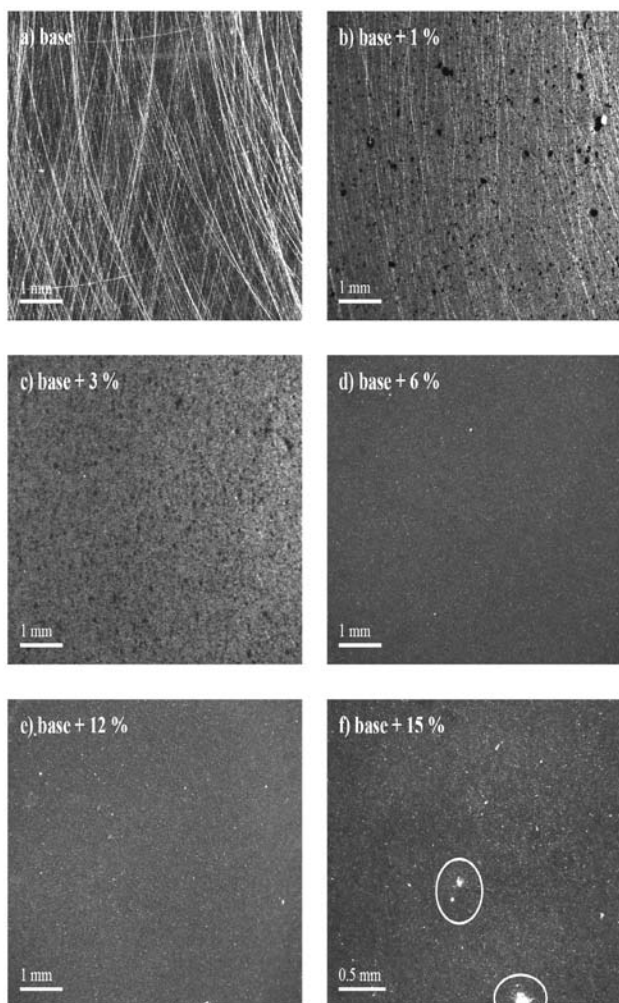


Fig. 2 LM images of the six investigated coatings, denoted as the base + vol. % of the MoS_2 nanotubes addition. (a) base, (b) base + 1 %, (c) base + 3 %, (d) base + 6 %, (e) base + 12 %, (f) base + 15 %. The magnification in the panel (f) is twice larger than in the other panels. White spots encircled in the panel (f) are due to light reflection.

The LM results show that the MoS_2 nanotubes disperse homogeneously over the nanocomposite coating at the concentration level of 6 % and higher. At 6 %, the coating is already totally opaque, whereas 15 % nanotube addition causes the shiniest surface.

B. SEM Characterization

The SEM imaging of the coatings was performed on their top surface and the cross section. Representative images of the base + 6 % coating are shown in Fig. 3. The cross section image in Fig. 3a shows good dispersion of the nanotubes at the level of isolated tubes individually coated with polymer. Homogeneous dispersion and good adhesion of the polymer to the nanotubes are in favor of efficient transfer of the external stresses to the nanotube system in the composite reinforcement application. The image of the top surface (Fig. 3b) shows excellent surface finish with negligible roughness on the 10 μm scale.

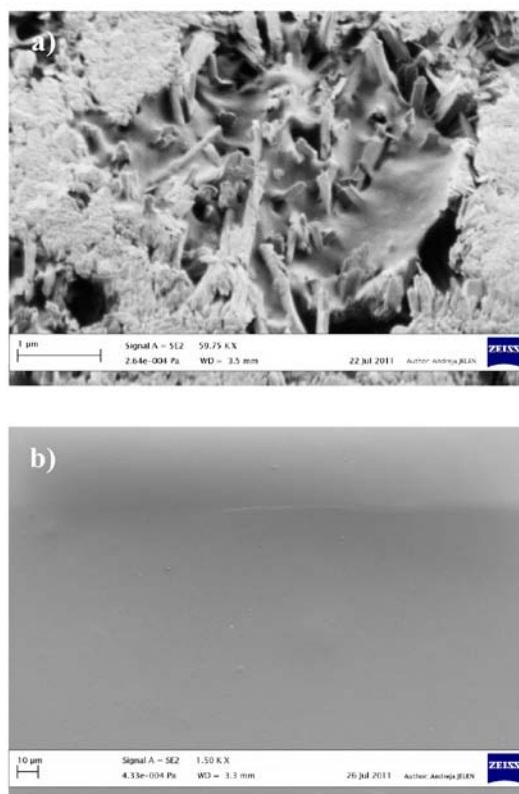


Fig. 3 SEM images of the base + 6 % coating: (a) cross section, (b) top surface.

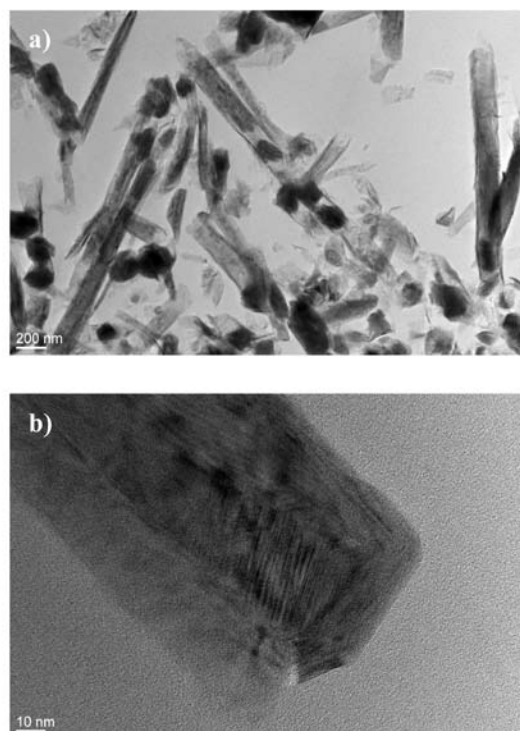


Fig. 4 (a) TEM image of the base + 12 % coating, showing fullerene-like MoS_2 nanoparticles inside the MoS_2 "mama-tubes". (b) Detail of the MoS_2 nanotube on a 10 nm scale, showing its crystallinity.

C. TEM Characterization

The TEM images of the base + 12 % coating (to be considered representative of all coatings) are shown in Fig. 4. On the scale of several 100 nm (Fig. 4a) we observe that some MoS_2 nanotubes contain nanoparticles inside, observed as dark spherical-like spots. Such tubes are known as "mama-

tubes" [13, 14] and contain lumps of the same material, MoS₂ fullerene-like nanoparticles in this case. The hollow nanotubes thus act as nanopods. Fullerenes are not observable in all nanotubes. In some cases fullerenes have fallen out of the tubes and form constituting part of the nanocomposite. It is these MoS₂ fullerene-like nanoparticles that act as the super shock absorbers [9], indicating that our nanocomposite coatings might possess the shock-absorbing property. In Fig. 4b, the crystallinity of the MoS₂ nanotube can be observed on the nm scale.

The above presented characterization of the nanocomposite coatings with LM, SEM and TEM microscopy techniques has shown that the MoS₂ nanotubes disperse homogeneously and isotropically within the polymer matrix to the level of isolated tubes individually coated with polymer. SEM imaging of the nanocomposite cross section indicates good adhesion of the nanotubes to the polymer matrix. Together with superior mechanical properties of the MoS₂ nanotube fillers and the presence of fullerene-like MoS₂ nanoparticles, this makes the MoS₂-polymer nanocomposite promising candidate for the reinforcement application.

IV. DYNAMIC MECHANICAL ANALYSIS OF THE NANOCOMPOSITE

DMA is a technique suitable for studying viscoelastic behavior of polymers. A sinusoidal displacement (strain ε) is applied to the material and the resulting force (stress σ) is measured. For a perfectly elastic solid, the strain and stress are in phase. For a purely viscous fluid, there is a 90° phase lag of strain with respect to stress. Viscoelastic polymers are characterized by a phase lag somewhere in between these values.

For sinusoidal stress $\sigma = \sigma_0 \sin(\omega t + \delta)$ and strain $\varepsilon = \varepsilon_0 \sin \omega t$, where δ is the phase lag, the tensile storage modulus E' , the loss modulus E'' and the $\tan \delta$ are defined as

$$E' = \frac{\sigma_0}{\varepsilon_0} \cos \delta, \quad (1)$$

$$E'' = \frac{\sigma_0}{\varepsilon_0} \sin \delta, \quad (2)$$

$$\tan \delta = \frac{E''}{E'}. \quad (3)$$

The storage modulus E' measures the stored energy, representing the elastic portion, whereas the loss modulus E'' measures the energy dissipated as heat due to internal friction, representing the viscous portion. One important application of DMA is the measurement of glass transition temperature T_g of polymers. Above T_g , the material has rubbery properties and the stiffness of the material drops dramatically with an increase in viscosity. At T_g , the storage modulus decreases strongly and the loss modulus reaches a maximum. Incorporation of reinforcing fillers into the polymer generally changes T_g and increases the storage modulus at an expense of limiting the loss tangent peak height.

DMA experiments were performed on TA Instruments Q800 apparatus in the temperature range from -50 °C to 100 °C. Testing was done in tensile mode. Coatings samples were cut in the shape of ribbons with lengths around 20 mm and widths from 4 to 5 mm. The starting clamping length was from 8.5 to 10 mm. The clamping stress was 5 psi and the load was 125 % of the drive force. In this way, the samples were flat

and leveled during the whole experiment, making no folds when exposed to sinusoidal deformation. The length of the samples was measured constantly during the tests. At the starting temperature, the length was measured firstly and this was the clamping length. At each temperature, the momentary length was used for the modulus correction because of heating. Therefore, the modulus values do not base on the clamping length, but on momentary length and computer calculations, assuring more accurate values of the modulus. The DMA tensile test was performed at $\nu = 1$ Hz frequency and 10 μm deformation amplitude.

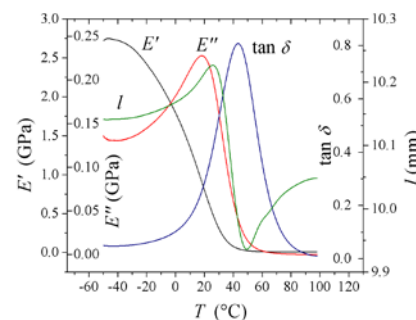


Fig. 5 (Color online) Viscoelastic properties of the base coating determined by DMA in the temperature range between -50 and 100°C: the storage modulus E' , the loss modulus E'' , the $\tan \delta$ and the length l .

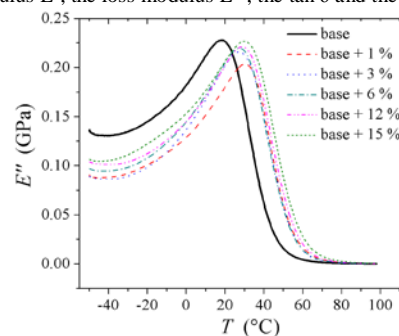


Fig.6 (Color online) Temperature-dependent loss modulus E'' of the investigated coatings. The samples are denoted as the base + vol. % of the MoS₂ nanotubes addition

A. Viscoelastic Properties of the Base Coating

In the first set of the DMA experiments, viscoelastic properties of the base coating were defined as a function of temperature. The resulting storage modulus E' , loss modulus E'' , $\tan \delta$ and length l are shown on the same graph in Fig. 5. The maximum in E'' occurs at the temperature 18.4 °C, which represents the glass transition temperature T_g of the base at the employed frequency of 1 Hz. The storage modulus drops drastically as the material goes from the hard glassy to a rubbery state, from the maximum value of $E'_{\text{max}} = 2.75$ GPa at $T = -50$ °C to the value at T_g of $E'_{T_g} = 0.88$ GPa, whereas the RT value at $T = 25$ °C is $E'_{\text{RT}} = 0.53$ GPa. The loss modulus value at T_g amounts $E'_{T_g} = 0.23$ GPa, whereas the RT value is $E'_{\text{RT}} = 0.21$ GPa. The $\tan \delta$ curve shows maximum at the temperature $T_\delta = 42.9$ °C and the maximum phase lag at T_δ amounts $\delta_{T_\delta} = 39^\circ$. T_δ defines one end of the temperature range over which the polymer can be used, called the operating range of the polymer. If the strength and stiffness are required, T_δ is the upper limit, whereas for rubber-like application, it is the lower-limit temperature. Considering the reinforcement application, the operating range of the base is roughly above 0 °C. At temperatures below 0 °C, the material is brittle and not resistant towards impact load, whereas at temperatures above T_δ it becomes gradually too soft due to increased viscosity. The temperature-dependent length l first expands on

approaching T_g from below and reaches its maximum value at $T_{l_{\max}} = 25.8^\circ\text{C}$, where l_{\max} is 0.9 % longer than the initial length l_o at $T = -50^\circ\text{C}$. This is followed by shrinkage until $T_{l_{\min}} = 48.5^\circ\text{C}$, where the length reaches its minimum value l_{\min} that is 2.9 % shorter than the initial length. Upon further heating, the viscosity component causes continuous lengthening until the end of the test. The discussion of the temperature dependencies of E' , E'' , $\tan \delta$ and l will be given in the following paragraphs, by comparing properties of the base to those of the nanocomposites with the MoS_2 addition. The values of T_g , E'_{\max} , E'_{T_g} , E'_{RT} , E''_{T_g} , E''_{RT} , T_{δ} , δT_{δ} , $T_{l_{\max}}$, $T_{l_{\min}}$, $(l_{\max}-l_o)/l_o$ and $(l_o-l_{\min})/l_o$ are also collected in Table 1.

B. Change of T_g and the Loss Modulus E'' of the Nanocomposite Coatings

The T_g of the nanocomposite coatings was determined from the maximum in the loss modulus E'' . The temperature-dependent E'' of all coatings is shown in Fig. 6. The MoS_2 nanotube addition has shifted the glass transition to higher temperatures. Nanotubes act as stiff cross-points, which impede segmental oscillations of the polymer matrix, so that more thermal energy is needed to excite relaxational motions. In Fig. 6 we observe that the maximum in E'' and the associated T_g of the nanocomposite coatings have shifted from the base value of 18.4°C into the range $26 - 30^\circ\text{C}$ (Table 1).

The increased T_g values are randomly scattered within the above temperature range, so that no direct correlation to the concentration of MoS_2 nanotubes can be claimed. The average

glass temperature of the nanocomposites is $T_g = 28.4 \pm 1.8^\circ\text{C}$ for the employed MoS_2 concentration range between 1 % and 15 %, which is by about 10°C higher than the base value. The loss modulus values E''_{T_g} and E''_{RT} of all coatings are given in Table 1. The differences in the loss modulus maximum value E''_{T_g} between the nanocomposite coatings and the base and between the nanocomposite coatings themselves are only marginal.

C. The Storage Modulus E' of the Nanocomposite Coatings

The temperature-dependent storage modulus E' of all coatings is shown in Fig. 7. Within the temperature range suitable for mechanical loading (roughly above 0°C and before the material gets too soft), the MoS_2 addition has resulted in higher modulus at a given temperature for all concentrations of the nanotubes, i.e., the nanocomposites are generally stiffer. At RT, the E'_{RT} value of the nanocomposites

has increased from the base value $E'_{RT} = 0.53 \text{ GPa}$ into the range $0.93 - 1.18 \text{ GPa}$ (Table 1), thus by factors $1.8 - 2.2$, so that the storage modulus has practically doubled by the MoS_2 addition. The base + 15 % coating is the stiffest ($E'_{RT} = 1.18 \text{ GPa}$), as can be expected for the highest addition of the MoS_2 nanotubes.

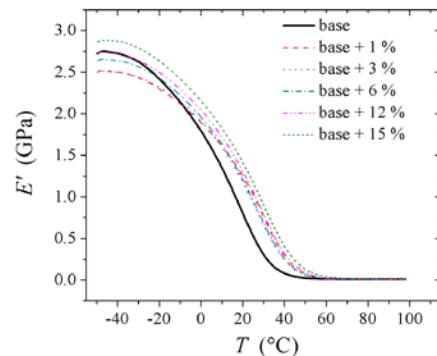


Fig. 7 (Color online) Temperature-dependent storage modulus E' of the investigated coatings. The samples are denoted as the base + vol. % of the MoS_2 nanotubes addition.

The storage modulus values at the glass temperature, E'_{T_g} , of the nanocomposite coatings with different MoS_2 concentrations show only marginal differences, being in the range $0.80 - 0.91 \text{ GPa}$ (Table 1). The base value (0.88 GPa) also falls in this range. This demonstrates that, within the temperature range suitable for mechanical loading, the temperature-dependent E' curves of the nanocomposites are roughly translated on the temperature scale by about 10°C to higher temperatures with respect to the base curve, which is by the amount of the T_g shift due to the nanotubes addition.

The maximum value of the storage modulus, E'_{\max} , at $T = -50^\circ\text{C}$ deeply in the glass phase shows the following interesting variation with the MoS_2 concentration (Table 1). Firstly, the stiffness of the nanocomposites monotonously increases with the nanotubes concentration. However, the 1, 3 and 6 % nanotubes addition slightly decreases the modulus E'_{\max} , below the base value of 2.75 GPa . For the 12 % addition E'_{\max} becomes equal to the base value, whereas it becomes larger (2.88 GPa) only for the highest concentration of 15 %. Therefore, adding MoS_2 nanotubes in lower concentrations even decreases the nanocomposite stiffness below the base value deeply in the glass phase and the reinforcement effect in the entire investigated temperature range from -50°C to 100°C is only present for high enough

sample	T_g ($^\circ\text{C}$)	storage modulus E'			loss modulus E''		$\tan \delta$		length			
		E'_{\max} (GPa)	E'_{T_g} (GPa)	E'_{RT} (GPa)	E''_{T_g} (GPa)	E''_{RT} (GPa)	T_{δ} ($^\circ\text{C}$)	δT_{δ} ($^\circ$)	$T_{l_{\max}}$ ($^\circ\text{C}$)	$T_{l_{\min}}$ ($^\circ\text{C}$)	$(l_{\max}-l_o)/l_o$ (%)	$(l_o-l_{\min})/l_o$ (%)
base	18.4	2.75	0.88	0.53	0.23	0.21	42.9	39.0	25.8	48.5	0.9	2.9
base + 1 %	30.3	2.51	0.80	1.04	0.20	0.19	53.6	39.6	36.7	62.4	0.8	2.0
base + 3 %	26.8	2.51	0.86	0.93	0.21	0.22	55.0	45.6	35.0	63.9	0.9	3.8
base + 6 %	27.0	2.65	0.83	0.96	0.22	0.22	54.0	41.7	37.2	62.0	1.1	2.4
base + 12 %	28.5	2.74	0.86	1.05	0.22	0.22	55.8	40.0	38.1	65.1	0.9	2.1
base + 15 %	29.9	2.88	0.91	1.18	0.23	0.22	55.7	36.1	38.1	62.6	0.8	1.5

Table 1 The glass transition temperature T_g , the storage modulus E' (the maximum value E'_{\max} at $T = -50^\circ\text{C}$, the value at T_g , E'_{T_g} , and the RT value E'_{RT} at $T = 25^\circ\text{C}$), the loss modulus E'' (E''_{T_g} and E''_{RT}), the $\tan \delta$ parameters (the temperature T_{δ} of the $\tan \delta$ peak and the maximum phase lag δT_{δ}), and the length parameters (the maximum relative elongation $(l_{\max}-l_o)/l_o$ and contraction $(l_o-l_{\min})/l_o$, where l_o is the initial length at $T = -50^\circ\text{C}$, and the temperatures $T_{l_{\max}}$ and $T_{l_{\min}}$ of the maximum elongation/contraction).

nanotube concentration (above 12 %). At RT (and generally in the range suitable for mechanical loading), on the other hand, the addition of MoS₂ nanotubes in any concentration reinforces the composite coating, i.e., all nanocomposites are stiffer than the base.

D. The $\tan \delta$ of the Nanocomposite Coatings

The temperature-dependent $\tan \delta$ curves of the base and the nanocomposite coatings are shown in Fig. 8. $\tan \delta$ is an indicator of how efficiently the material can loose the energy due to molecular rearrangement and internal friction. At the $\tan \delta$ peak temperature T_δ , molecular bonds are breaking; enabling intense segmental oscillations within the polymer matrix and making the material loosen. The $\tan \delta$ peaks (and the associated T_δ) of the nanocomposite coatings are shifted to higher temperatures from the base value of $T_\delta = 42.9^\circ\text{C}$ into the range $53 - 56^\circ\text{C}$ (Table 1). There is again no pronounced correlation between the T_δ shift and the MoS₂ concentration,

so that an average $T_\delta = 54.8 \pm 1.2^\circ\text{C}$ of the nanocomposites can be defined. The shift of the T_δ temperature by $\Delta T_\delta \approx 11^\circ\text{C}$ upon the nanotubes addition is about the same as the shift of

the glass temperature ΔT_g and correlates well to the segmental motion obstruction by the nanotubes. Due to the T_δ shift by about 11°C , the temperature range suitable for mechanical loading of the nanocomposites has also extended to higher temperatures by the same amount. The maximum phase lag δ_{T_δ} of the nanocomposites obtained from the $\tan \delta$ peak value falls into the range $36 - 46^\circ$ (Table 1) with no direct correlation to the MoS₂ concentration. Since the base value (39°) also falls in this range, the nanotubes addition did not change the phase lag significantly.

E. The Length of the Nanocomposite Coatings

The temperature-dependent length of the base and the nanocomposite coatings is shown in Fig. 9. The lengths of all coatings are changing in a similar manner. In the low-temperature part of the experiment between -50°C and about 30°C , the samples are slightly stretching upon heating and the maximum length l_{\max} is observed in the glass transition area at a temperature $T_{l\max}$ somewhere between the peaks in E'' and $\tan \delta$. The stretching is caused by braking of the intermolecular bonds, the free volume increase and consequent loosening of the structure. After the structural relaxation in the glass transition area takes place, intermolecular forces are established again, the free volume is reduced and the material experiences slight contraction. The entropy is the highest in the most contracted state where the length reaches its minimum value l_{\min} at the temperature $T_{l\min}$ slightly higher than T_δ . At still higher temperatures, the viscous component causes further expansion of the material.

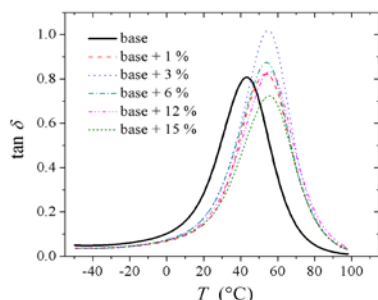


Fig. 8 (Color online) Temperature-dependent $\tan \delta$ curves of the investigated coatings. The samples are denoted as the base + vol. % of the MoS₂ nanotubes addition.

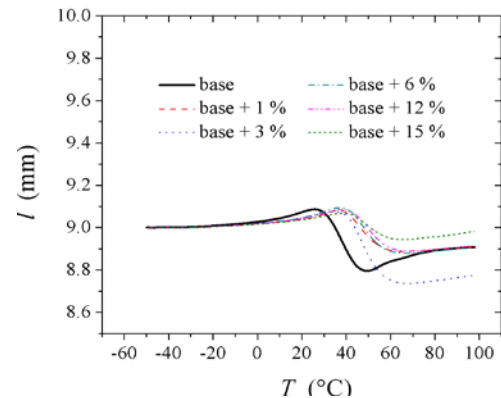


Fig. 9 (Color online) Temperature-dependent length l of the investigated coatings. The samples are denoted as the base + vol. % of the MoS₂ nanotubes addition.

Upon adding MoS₂ nanotubes to the polymer matrix, $T_{l\max}$ of the nanocomposites has shifted upwards from the base value of 25.8°C into the range $35 - 38^\circ\text{C}$ (Table 1) and the maximum relative elongation $(l_{\max} - l_o)/l_o$ with respect to the initial length l_o is in the range $0.8 - 1.1\%$ (Table 1). The base value (0.9%) also falls into this range. After the material contraction in the glass transition area, the $T_{l\min}$ values of the nanocomposites have shifted from the base value of 48.5°C into the range $62^\circ\text{C} - 65^\circ\text{C}$, and the maximum relative contraction $(l_o - l_{\min})/l_o$ is in the range $1.5 - 3.8\%$ (Table 1), where the base value (2.9%) also falls in this range. Nanotubes addition to the polymer matrix thus shifts the characteristic temperatures $T_{l\max}$ and $T_{l\min}$ to higher temperatures, whereas the maximum relative elongation and contraction are not affected significantly. There is again no noticeable correlation of $T_{l\min}$, $T_{l\max}$, l_{\min} and l_{\max} to the MoS₂ nanotubes concentration.

V. DISCUSSION AND CONCLUSIONS

DMA analysis of the nanocomposite coatings has shown the following changes of their viscoelastic properties with respect to the base coating. The MoS₂ nanotubes addition into the polymer matrix has shifted the glass transition temperature by $\Delta T_g \approx 10^\circ\text{C}$ towards higher temperatures. The $\tan \delta$ peak temperature T_δ , the temperature range suitable for mechanical loading, the temperatures $T_{l\max}$ and $T_{l\min}$ of the maximum elongation/contraction have shifted towards higher temperatures by about the same amount. These changes originate from the nanotubes incorporation into the polymer matrix, acting as stiff cross-points that impede segmental oscillations, so that more thermal energy is needed to excite internal motions in the nanocomposites. The main benefit of the MoS₂ nanotubes addition is a significant increase of the storage modulus E' within the temperature range suitable for mechanical loading, being at RT roughly a factor of 2 larger than E' of the base. The stiffness of the nanocomposites has thus increased quite significantly by the nanotubes addition. The coating with the highest MoS₂ concentration of 15% is the stiffest, with its E'_{RT} value being a factor 2.2 larger than that of the base. At low temperatures deeply in the glass phase of the polymer matrix, the reinforcement effect depends on the MoS₂ concentration. Slight reinforcement (an increase of the storage modulus E'_{\max} by about 5% from the base value) is observed only for the highest concentration of 15% , whereas at lower concentrations, E'_{\max} of the nanocomposites

is equal or even smaller than the storage modulus of the base. Therefore, adding MoS₂ nanotubes in lower concentrations decreases the nanocomposite stiffness below the base value deeply in the glass phase and the reinforcement effect in the entire investigated temperature range from -50 °C to 100 °C is only present for high enough nanotubes concentration (above 12 %). At RT (and generally in the range suitable for mechanical loading), on the other hand, the addition of MoS₂ nanotubes in any concentration reinforces the composite coating, i.e., all nanocomposites are stiffer than the base.

Comparing the reinforcement performance of our MoS₂-containing nanocomposite to some other known nanocomposites, we note that the nanocomposite of a nylon 6 matrix with montmorillonite (MMT) clay nanofillers shows similar degree of reinforcement [15]. The storage modulus of the nylon 6 matrix ($E = 2.75$ GPa) is the same as that of our base coating, whereas the storage modulus of the MMT nanofiller (178 GPa) is also comparable to that of the MoS₂ nanotubes [5]. The modulus increase of the nylon 6 nanocomposite containing 3 vol. % of the MMT nanofiller was reported to be by a factor 2.1, which is about the same as for our MoS₂-based nanocomposite. For the multi-walled carbon nanotubes mixed in different concentrations into different polymers (PMMA, PS, PC, PA6, nylon), the modulus increase was reported to be by factors between 1.1 and 3.1 (see Table 2 of ref. [2] and references therein), whereas for the single-walled carbon nanotubes the modulus increase was by factors between 1.6 and 3.5 (see Table 3 of ref. [2] and references therein). The reinforcement performance of our MoS₂-based nanocomposites with the modulus increase by a factor about 2 thus compares well to that of the carbon nanotubes- and the MMT-reinforced nanocomposites.

ACKNOWLEDGEMENT

We thank Dr. Kristina Žagar from J. Stefan Institute for her help in TEM experiments.

REFERENCES

- [1] See, for a review: D.R. Paul and L.M. Robeson, *Polymer* 49 (2008) 3187-3204, and references therein.
- [2] See, for a review: J.N. Coleman, U. Khan, W.J. Blau and Y.K. Gun'ko, *Carbon* 44 (2006) 1624-52, and references therein.
- [3] R. Tenne, *Colloids and Surfaces A: Physicochem. Eng. Aspects* 208 (2002) 83-92.
- [4] M. Remškar and A. Mrzel, *Vacuum* 71 (2003) 177-83.
- [5] Kis, D. Mihailovic, M. Remškar, A. Mrzel, A. Jesih, I. Piwonski, A.J. Kulik, W. Benoît and L. Forró, *Adv. Mater.* 15 (2003) 733-6.
- [6] L. Joly-Pottuz, F. Dassenov, M. Belin, B. Vacher, J.N. Martin and N. Fleischer, *Tribol. Lett.* 18 (2005) 477-85.
- [7] L. Rapoport, N. Fleischer and R. Tenne, *J. Mater. Chem.* 15 (2005) 1782-8.
- [8] M. Chhowalla and G.A. Amaratunga, *Nature* 407 (2000) 164-7.
- [9] Y.Q. Zhu, T. Sekine, Y.H. Li, W.X. Wang, M.W. Fay, H. Edwards, P.D. Brown, N. Fleischer and R. Tenne, *Adv. Mater.* 17 (2005) 1500-3.
- [10] J. Chen, S.L. Li and Z.L. Tao, *J. Alloys Compd.* 356-357 (2003) 413-7.
- [11] Zak, Y. Feldman, V. Lyakhovitskaya, G. Leiturs, R. Popovitz-Biro, E. Wachtel, H. Cohen, S. Reich and R. Tenne, *J. Am. Chem. Soc.* 124 (2002) 4747-58.
- [12] J. Chen, Z.L. Tao and S.L. Li, *Angew. Chem. Int. Ed.* 42 (2003) 2147-51.
- [13] M. Remškar, A. Mrzel, M. Viršek and A. Jesih, *Adv. Mater.* 19 (2007) 4276-8.
- [14] M. Remškar, M. Viršek and A. Mrzel, *Appl. Phys. Lett.* 95 (2009) 133122.
- [15] T.D. Fornes and D.R. Paul, *Polymer* 44 (2003) 4993-5013

